Desalination and Water Treatment
www.deswater.com

doi: 10.1080/19443994.2013.803342

52 (2014) 3497–3503
May

Taylor & Francis
Taylor & Francis Group

Preparation and characterization of nanoscale cadmium oxide using bovine serum albumin as green capping agent and its photocatalytic activity

Deepak Pathania[a,*], Sarita[a], Pardeep Singh[a], Sarita Pathania[b]

[a]*Department of Chemistry, Shoolini University of Biotechnology and Management Sciences, Solan 173212, Himachal Pradesh, India*
Tel. +91 1792308000; email: dpathania74@gmail.com
[b]*Department of Zoology, Safia Science College, Bhopal, MP, India*

Received 30 November 2011; Accepted 24 April 2013

ABSTRACT

Cadmium oxide nanoparticles were synthesized in aqueous phase at 70°C using bovine serum albumin (BSA) as the capping agent. X-ray diffraction, transmission electron microscopy, thermogravimetric analysis, and Fourier transform infra red techniques were used to characterize CdO nanoparticles. The average particle sizes of CdO nanoparticles were found to be ~14 nm. The polarity of the BSA capped CdO nanoparticles was determined using gel electrophoresis technique. The synthesized CdO nanoparticles were used as photocatalyst for methylene blue degradation. The photodegrdation of methylene blue was optimized under different reaction conditions such as catalyst loading, dye concentration, temperature, and pH. Methylene blue dye was completely decolorized in 70 min of irradiation time. CdO nanoparticles were effectively used as antibacterial agent to inhibit the growth of *Escherichia coli* bacteria.

Keywords: CdO nanoparticles; BSA; Photocatalytic activity; Methylene blue

1. Introduction

Nanoparticles have attracted steadily increasing interest due to their peculiar and fascinating properties, as well as their unique applications complementary to the bulk materials. Semiconductor-assisted photocatalysis has gained important place among various advanced oxidation methods for wastewater treatment. Nano-sized metal oxide suspension in liquid phase has a high solid to liquid contact area which is beneficial for a high rate of reaction. Nano-sized TiO_2 and ZnO are the most widely studied photocatalysts for environment remediation owing to their unique photocatalytic and antibacterial activities [1,2]. Manjula et al. explored antibacterial and photocatalytic activity of ZnO nanoparticles [3]. Xiong et al. investigated the mechanism of heterogeneous photocatalytic degradation using titanate nanotubes [4]. Karunakaran et al. utilized ZnO–TiO_2 nanocomposite for photocatalytic bacteria disinfection and cyanide detoxification under visible light [5]. However, poor adsorption of organic molecules onto catalyst surface has an adverse effect on photocatalyic process.

Currently, pectin/Fe_3O_4, magnenite/chitosan, hydroxyapetite/chitosan, pectin/ZnO, and chitosan/

*Corresponding author.

cellulose composites have been explored for adsorptional removal of dyes and heavy metals from aqueous phase. These biomolecules can also act as a shape directing agent to promote anisotropic growth and to increase adsorption capacity of metal oxides [5,6]. Bovine serum albumin (BSA) is a versatile carrier protein with both hydrophobic and hydrophilic functionalities. In precedent work, BSA was used as capping agent to prepare CdO nanoparticles with enhanced photocatalytic activity for dye degradation.

Recently, semiconductor mediated photocatalysis has emerged as an alternative to conventional treatment methods involving generation of hydroxyl radicals that oxidize a broad range of organic pollutants quickly and non-selectively. Upon illumination of semiconductor particles with artificial light greater than band-gap energy ($h\upsilon > E_g = 2.5$ eV), electron-hole pairs are (e_{CB}^-/h_{VB}^+) are generated (Fig. 1). The photogenerated holes are able to migrate to the hydroxylated surface of catalyst and can create the highly reactive radical $^{\cdot}OH$ (standard redox potential 2.8 eV). Secondly, dye molecules act as a sensitizer by the absorption of visible light. The transfer of photogenerated electrons to dissolved oxygen ultimately leads to the enhanced formation of hydroxyl radicals [7–8]. Dye molecules are mainly oxidized by $OH^{\cdot}$ to degraded products. Methylene blue dye is extensibly used in textile industry, and is resistant to bio-degradation. The present study was aimed at the synthesis of BSA capped CdO nanoparticles at 70˚C. The synthesized nanoparticles were effectively used for the removal of methylene blue dye from aqueous phase in the presence of artificial visible light.

2. Materials and methods

2.1. Materials

All the chemicals used were of analytical grade. BSA and $CdSO_4$ were purchased from Sigma Aldrich Company (India) and used without further purification. CH_3COOH and NaOH were obtained CDH Company, India. Methylene blue was obtained from Sigma Aldirch Company (India). The double-wall cylinder (borosilicate glass), magnetic stirrer, digital thermostatic water bath, pH-meter, thermometer, halogen lamp, and aluminum reflectors were used to construct photoreactor.

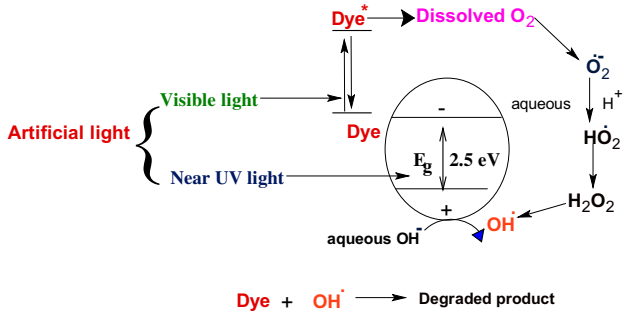

Fig. 1. Mechanism of photocatalytic degradation.

2.2. Synthesis of cadmium oxide nanoparticles

Different solutions were prepared by dissolving 1 M BSA (10 ml), 0.1 M $CdSO_4$ (50 ml), 0.1 M CH_3COOH (5 ml), and 0.1 M NaOH (100 ml) with double distilled water. $CdSO_4$ solution was added to bovine serum solution with continuous stirring for 15 min at room temperature. To the resulting mixture, CH_3COOH solution was added with constant stirring followed by the addition of NaOH solution. The obtained solution was stirred for three hours at 70˚C to obtain precipitates. The mixture was centrifuged at 10,000 rpm to obtain brown precipitates. The obtained precipitates were washed several times with ethanol and distilled water to remove impurities. Finally, precipitates were heated at 250˚C for 5 h to obtain brownish color cadmium oxide nanoparticles.

2.3. Instrumentation

Thermal analysis of CA/ZPNC was performed on thermogravimetric analyzer (NETZSCH TG 209 F1). Thermal analyses were determined in temperature range of 0–1000˚C. X-ray diffraction (XRD) data were recorded on Phillips, PW 1,148/89 X-ray diffractometer using CuKα radiation having the wavelength of 1.5418 Å. Fourier transformer infrared spectra (FTIR) were obtained using Perkin Elmer spectrometer (Spectrum 400, USA) in the wavelength range 400–4,000 cm^{-1}. Scanning electron microscope (Quant-250, model 9,393) was used to explore surface morphology. The microstructure of CA/ZPNC was analyzed using Transmission electron microscope (Tecnai 20 G2 Plate/CCD Camera). CR concentration was determined using UV–Visible spectrophotometer (Systronics 117).

2.4. Photocatalytic experiments

The photocatalytic experiments were carried out in an indigenously designed and developed open batch reactor having double-wall borosilicate glass cylinder (ht. 7.5 cm × dia. 6 cm) (Fig. 2). The double-wall cylinder was equipped with magnetic stirrer and thermostatic water circulation arrangement to keep temperature in the range of 30 ± 0.3˚C comparable to

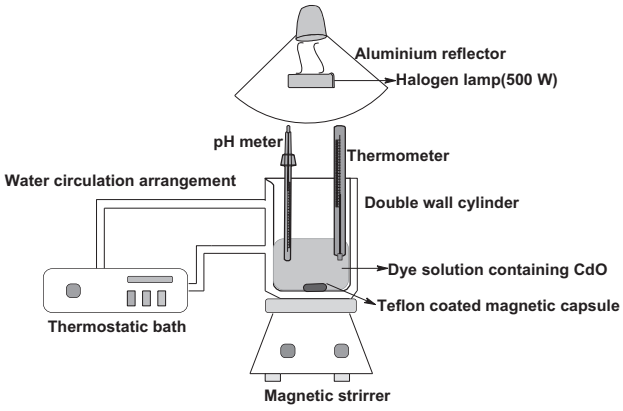

Fig. 2. Schematic representation of photoreactor.

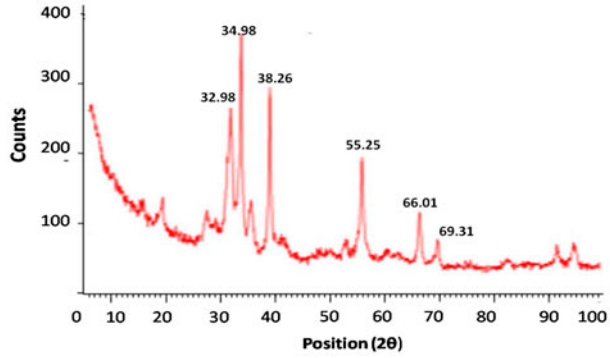

Fig. 3. XRD pattern of CdO nanoparticles.

ambient reaction conditions. The irradiation was carried out using 500 W halogen lamp (Philips, India) surrounded with aluminum reflectors in order to avoid loss of irradiation. The radiations emitted by halogen lamp were comparable to sunlight. After stirring for ten minute, dye solution containing CdO suspension was placed in dark for half an hour in order to establish equilibrium between adsorption and desorption phenomenon on the surface of photocatalyst. Now, dye solution containing CdO suspension was stirred magnetically to insure complete suspension of catalyst particle with simultaneous exposure to visible light. At specific time intervals, aliquot (2 ml) was withdrawn and centrifuged for 2 min to assess the extent of decolorization photometrically. Changes in absorption spectra were recorded at 653 nm on double-beam UV–vis spectrophotometer. The decolorization efficiency was calculated using following equation:

$$\% \text{ Efficiency} = \frac{C_0 - C}{C_0} \times 100 \quad (1)$$

where C_0 and C are the initial absorbance and instantaneous absorbance of dye solution.

3. Results and discussion

3.1. Characterization of CdO nanoparticles

Fig. 3 depicts XRD pattern of CdO nanoparticles. The spectrum shows the diffraction peaks at 2 θ values of 32.98, 34.98, 38.26, 55.25, 66.01, and 69.31 matching with 111, 200, 220, 311, and 222 of cubic CdO. This indicates the formation of CdO nanoparticles with excellent crystallinity [9]. The peak broadening in the XRD pattern indicates that small nanocrystals are present in the sample. The crystallite size of BSA capped CdO was determined using Debye Scherer formula was found to be 100 nm.

Transmission electron microscopy (TEM) results confirm the formation of BSA capped CdO naoparticles (Fig. 4). The smooth morphology of particles was due to predominant growth of CdO nanoparticles capped with BSA. The dark region in the TEM images is due to deposition of BSA to CdO nanoparticles.

The IR spectra of CdO nanoparticles showed the strong absorption peak at 618.14 cm^{-1} correspond to Cd–O stretching. The absorption peaks at 3464.27, 2924.83, and 1592.54 cm^{-1} are assigned to the stretching vibration of –OH, amide A (mainly –NH stretching vibration), and amide (the coupling of bending vibrate of N–H and stretching vibrate of C–N) bands, respectively. These results indicate that the nanoparticles are coated with BSA. The remaining peaks at 2853.55 and 1108.65 cm^{-1} are assigned to the C–H aliphatic stretching and C–O stretching, respectively [10].

Fig. 5 shows the results of thermogravimetric analyses (TGA) of CdO nanoparticles. A known weight of

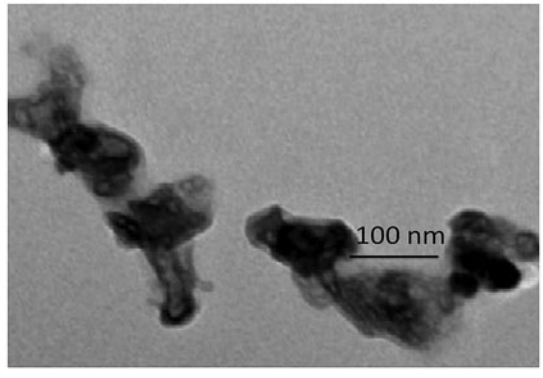

Fig. 4. TEM image of CdO nanoparticles at 200,000 magnification.

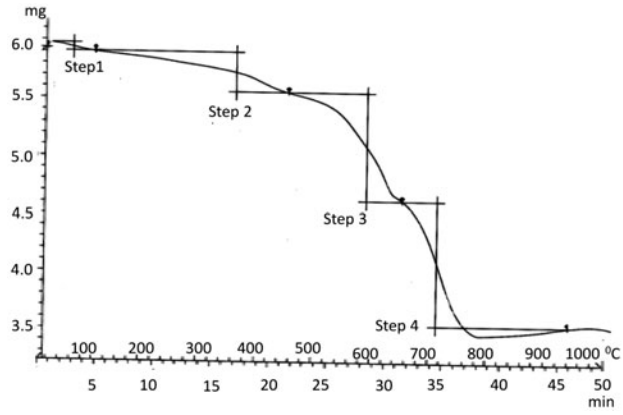

Fig. 5. TGA curve of CdO nanoparticles.

the each sample was taken into silica crucible for TGA analysis in air with temperature range of 50–700°C. The heating rate of sample was 10°C min^{-1} and was scanned for 60 min. In the second step, the total weight loss of 17.66% indicates the decomposition of organic matter mainly BSA. This further signifies that 17.66% of the total weight of the sample was BSA present in BSA capped CdO nanoparticles, a weight loss of 18.0499% in the range of 650–750°C. TGA analyses indicate that BSA capped CdO nanoparticles are stable up to 650°C.

The polarity of BSA capped CdO nanoparticles was determined by using gel electrophoresis technique. CdO nanoparticles show a displacement towards the positively charged electrode under the applied potential, suggesting that the surfaces of BSA capped CdO nanoparticles are predominantly negatively charged.

3.2. Photocatalytic degradation of MB

To explore the photocatalytic activity of CdO nanoparticles, the degradation of MB dye was investigated in slurry batch reactor under artificial visible radiations. The degradation efficiency is maximal at 350 mg/100 ml of catalyst loading (Fig. 6). The increased rate constant of VBB with higher catalyst loading is attributed to increment in the active sites available on the surface of catalyst for the reaction, which enhance the rate of radical formation of hydroxyl radicals and superoxide radicals [11,12]. The optimal concentration of MB was found to be 5×10^{-5} mol dm^{-3} (Fig. 7).

The degradation of dye as a function of reaction pH is shown in Fig. 8. The degradation of dye is maximal at pH value 6. At a higher pH value, adsorption of cationic dye on the surface of CdO increases. However, upon treatment with strong alkaline solutions, metal oxides form metalhydroxides [13]. These

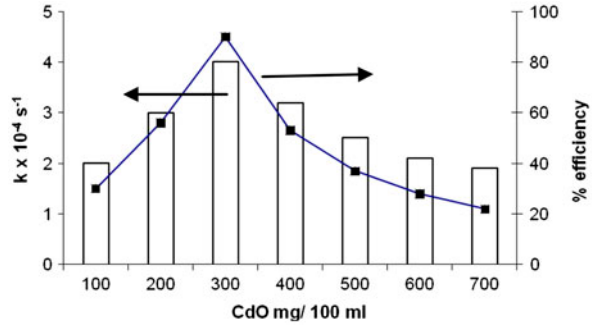

Fig. 6. Effect of catalyst loading: [MB] = 5.0×10^{-5} mol dm^{-3}, intensity = 56×10^3 lux, temperature = 30 ± 0.3°C, and pH = 6.0.

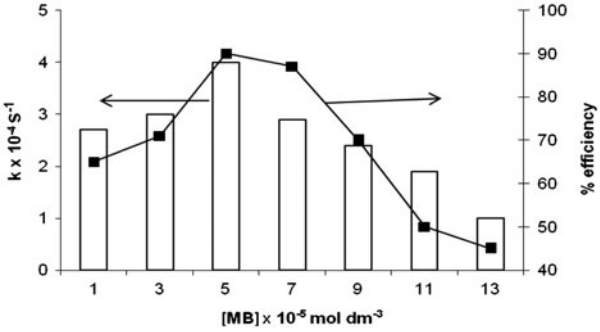

Fig. 7. Effect of MB concentration: [MB] = 5.0×10^{-5} mol dm^{-3}, CdO = 300 mg/100 ml, irradiation intensity = 56×10^3 lux, temperature = 30 ± 0.3°C, and pH = 6.0.

factors are responsible for optimum value of photodegradation of neutral red at pH 6.

The influence of temperature was studied in the range 30–55°C (Fig. 9). The rate constant is found to increase (3.07×10^{-4} s^{-1} to 3.7×10^{-4} s^{-1}) with the increase in temperature from 30 to 35°C. However, a further increase in temperature reduces the rate constant. The increased temperature tends to reduce electron-hole recombination. However, an increment in temperature also decreases the solubility of oxygen in water [14]. Both above-mentioned conflicting factors have been equipoised at 45°C. Significant amount of solution was evaporated at higher temperature.

Fig. 10 depicts photodegradation of methylene blue under different reaction conditions. There was considerable degradation of MB upon artificial visible light exposure in the presence of CdO. MB dye was completely decolorized in 60 min. In case of solar light, 90% of dye is decolorized in 60 min. No significant changes in dye absorbance were recorded either in the absence of photocatalyst or visible artificial radiations.

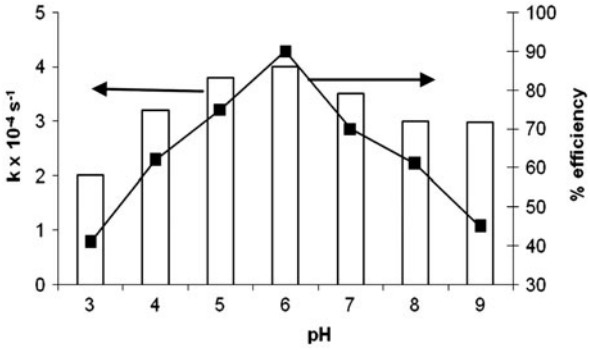

Fig. 8. Effect of pH: [MB] = 5.0×10^{-5} mol dm^{-3}, CdO = 300 mg/100 ml, irradiation intensity = 56×10^3 lux, and temperature = 30 ± 0.3 °C.

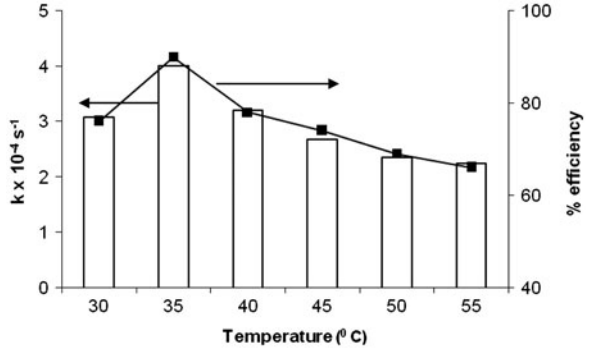

Fig. 9. Effect of temperature: [MB] = 5.0×10^{-5} mol dm^{-3}, CdO = 300 mg/100 ml, irradiation intensity = 56×10^3 lux, and pH = 6.0.

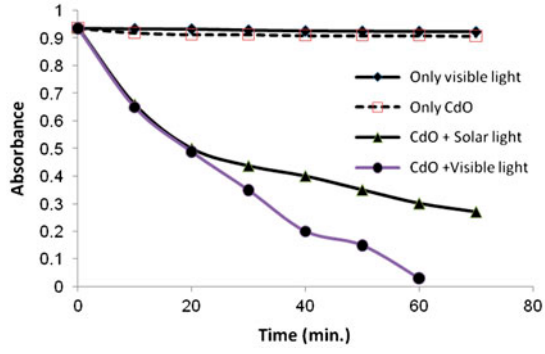

Fig. 10. Photocatalytic degradation of MB under different reaction conditions:[MB] = 5.0×10^{-5} mol dm^{-3}, CdO = 300 mg/100 ml, irradiation intensity = 56×10^3 lux, temperature = 30 ± 3 °C, and pH = 6.

3.3. Kinetics and mechanism of MB photodegradation

The dependencies of the rate of dye degradation on its concentration as a function of irradiation time have been described well by Langmuir-Hinshelwood pseudo-first-order kinetic model [15,16].

$$-\frac{dC}{dt} = kt \tag{2}$$

where C is the initial dye concentration at a given time t. Eq. (3) can be solved by integration between the limits (0, C_0) and (t, C) for photocatalytic reaction time and dye concentration. The following integrated expression has

$$\ln\left(\frac{C_0}{C}\right) = kt \tag{3}$$

been obtained. From Fig. 11, the linear fit ($R^2 = 0.96$) between ln (C_0/C) and irradiation time can be approximated as pseudo-first-order kinetics.

Valence band holes (h_{VB}^+) and conduction band electrons (e_{CB}^-) are generated when aqueous ZnO suspension is irradiated with visible light energy greater than the its band-gap energy ($E_g = 2.8$ eV). These electron-hole pairs interact separately with other molecule. Valence band holes (h_{VB}^+) react with surface bound H_2O or OH^- to produce hydroxyl radical ($OH^{\cdot}$). Valence band holes can also oxidize organic molecule. Conduction band electrons (e_{CB}^-) reduce molecular oxygen to generate superoxide radicals as shown in Eqs. (5)–(8) [17–20].

$$CdO + h\nu_{visible} \rightarrow CdO(h_{VB}^+) + e_{CB}^- \tag{4}$$

$$CdO\ (h_{VB}^+) + H_2O \rightarrow CdO + H^+ + OH^{\cdot} \tag{5}$$

$$CdO\ (h_{VB}^+) + OH^- \rightarrow CdO + OH^{\cdot} \tag{6}$$

$$CdO\ (e_{CB}^-) + O_2 \rightarrow CdO + O_2^{\cdot -} \tag{7}$$

Sensitization of dye by visible light causes the excitation of dye molecule to singlet or triplet state, subse-

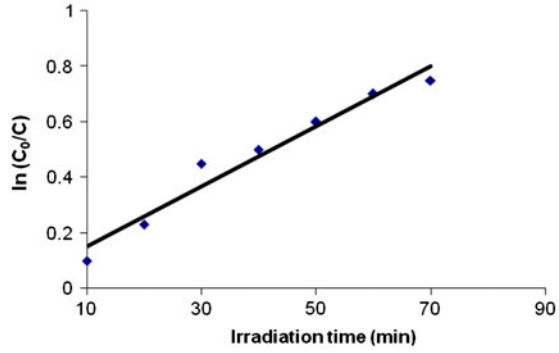

Fig. 11. Pseudo-first-order photocatalytic degradation: MB] = 5.0×10^{-5} mol dm^{-3}, CdO = 300 mg/100 ml, irradiation intensity = 56×10^3 lux, temperature = 30 ± 0.3 °C, and pH = 6.

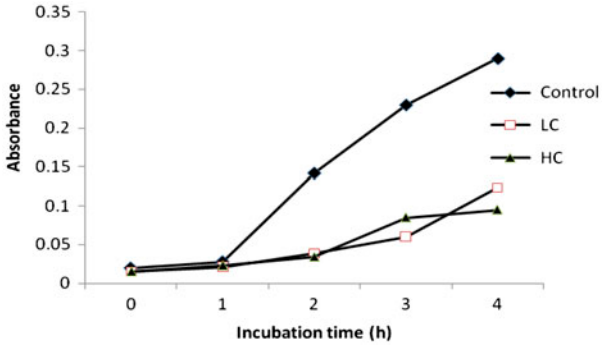

Fig. 12. Antibacterial properties of CdO nanoparticles: LC = low concentration of CdO. HC = High concentration of CdO.

Visible spectrophotometer. Fig. 12 shows the growth curve of *E. coli* bacteria in the presence of CdO nanoparticles with respect to control. The high concentration of CdO nanoparticles inhibits the bacteria growth to more extent as compared to low concentration of CdO nanoparticles. The mechanism for the inhibition of *E. coli* bacteria culture is same as described in case of CdO nanoparticles. It has been observed that the CdO nanoparticles are able to inhibit the growth of *E. coli* bacteria. The inhibition of *E. coli* bacteria was probably due to damage of cell membrane of *E. coli* by Cd^{2+} ions and by the interaction with intercellular content of *E. coli* [22].

Table 1
Comparison of different photocatalytic sysytems for dye decolorization

Photocatalytic system	Dye	Decolorization time (min)	Reference
TiO_2/visible light	Ponceau 4R	120	19
CuS/sunlight	Methylene blue	90	20
BiOI/visible light	Acid orange II	120	21
Zero valent iron/visible light	Rhodamine B	180	22
BIOCl/visible light	Methylene green	120	23
CuS/visible light	Mthylene blue	60	Present study

quently followed by electron injection from excited dye molecule onto conduction band of semiconductor particles (Eqs. (9), and (10)). Methylene blue dye was subsequently degraded mainly by hydroxyl radicals [17–20].

$$MB + h\nu_{visible} \rightarrow {}_1MB^* \text{ or } {}_3MB^* \quad (8)$$

$${}_1MB^* \text{ or } {}_3LFY^* + CdO \rightarrow MB^{+\cdot} + CdO(e^-_{CB}) \quad (9)$$

$$MB^{+\cdot} + OH^- \rightarrow MB + OH^{\cdot} \quad (10)$$

$$MB^{+\cdot} + O_2^{-\cdot} \rightarrow \text{Degradation products} \quad (11)$$

$$MB + OH^{\cdot} \rightarrow \text{Degradation products} \quad (12)$$

3.4. Antibacterial properties of CdO nanoparticles

The antibacterial properties of CdS nanoparticles were determined against gram negative *Escherichia coli* bacteria culture by growth curve method [21]. The optical density of these solutions and control (i.e. NB and bacteria culture without CdS nanoparticles) were measured at regular time intervals (60 min) using UV–

4. Conclusion

The present study outlines synthesis of cadmium oxide nanoparticles under ambient reaction conditions using BSA as a green capping agent at 70°C. The morphology and surface composition of synthesized nanoparticles were investigated XRD, TEM, FTIR, TGA, and gel electrophoresis. The size of synthesized nanoparticles was found to be 100 nm. The photocatalytic and antibacterial activity of CdO nanoparticles were investigated. The photodegradation of MB was optimal at 350 mg/100 ml of catalyst loading. The color abatement was maximal at pH 6. On comparing with existing photocatalytic system in Table 1, BSA capped CdO has proven as an efficient photocatalyst under chosen reaction conditions. CdO nanoparticles have shown antibacterial properties against *E.coli* bacteria. From precedent study, it can be concluded that BSA capped CdO mediated degradation of methylene blue promises to be a versatile, economic, environmentally benign and efficient method of wastewater treatment, if all parameter are properly optimized.

Acknowledgment

Authors are grateful to Vice Chancellor, Shoolini University, Solan HP, India for his support. Authors are thankful to Directors of SAIF Laboratory Panjab

University, Chandigarh, India and NIPER, Mohali, Punjab, India for providing spectral analysis facility.

References

[1] D. Beydoun, R. Amal, L. Low, S. McEvoy, Role of nanoparticles in photocatalysis, J. Nanopart. Res. 1 (1999) 439–458.
[2] G. Bizhou, Z. Jun, L. Ping, K. Xianghong, H. Qiang, Study on degradation behavior of N, N-dimethylacetamide by photocatalytic oxidation in aqueous TiO2 suspensions, Desalin. Water Treat. 42 (2012) 274–278.
[3] G. Manjula Nair, M. Nirmala, K. Rekha, A. Anukaliani, Structural, optical, photo catalytic and antibacterial activity of ZnO and Co doped ZnO, Mater. Lett. 65 (2011) 1797–1800.
[4] L. Xiong, W. Sun, Y. Yang, C. Chen, J. Ni, Heterogeneous photocatalysis of methylene blue over titanate nanotubes: Effect of adsorption, J. Colloid Interface Sci. 356 (2011) 211–216.
[5] C. Karunakaran, G. Abiramasundari, P. Gomathisankar, G. Manikandan, V. Anandi, Preparation and characterization of ZnO–TiO_2 nanocomposite for photocatalytic disinfection of bacteria and detoxification of cyanide under visible light, Mater. Res. Bull. 46 (2011) 1586–1592.
[6] R. Rakhshaee, M. Panahandeh, Stabilization of a magnetic nano-adsorbent by extracted pectin to remove methylene blue from aqueous solution: A comparative studying between two kinds of cross-likened pectin, J. Hazard. Mater. 189 (2011) 158–166.
[7] L. Wang, A. Wang, Adsorption properties of Congo red from aqueous solution onto surfactant modified montmorillonite, J. Hazard. Mater. 147 (2007) 979–985.
[8] D. Chatterjee, S. Dasgupta, Visible light induced photocatalytic degrdation of organic pollutants, J. Photochem. Photobiol. C 6 (2005) 186–2005.
[9] B. Pare, S.B. Jonnalgada, H. Tomar, P. Singh, V.W. Bhagwat, ZnO assisted photocatalytic degradation of acridine orange in aqueous solution using visible irradiation, Desalination 232 (2008) 80–90.
[10] M. Manickathai, K.S. Viswanathan, M. Alagar, Synthesis and characterization of CdO and CdS nanoparticles, Indian J. Pure Appl. Phys. 46 (2008) 561–564.
[11] J. Mohan, In: Organic Spectroscopy, Principle and Applications, 2nd ed., Narosa Publication, New Delhi, 2005, pp. 76–79.
[12] K.V. Kumar, K. Porkodi, A. Selvaganapathi, Constrain in solving Langmuir–Hinshelwood kinetic expression for the for the photocatalytic degradation of auramine O aqueous solutions by ZnO catalyst, Dyes Pigm. 75 (2007) 246–249.
[13] M.A. Behnajady, N. Modirshahla, R. Hamzav, Kinetic study on photocatalytic degradation of C.I. Acid Yellow 23 by ZnO photocatalyst, J. Hazard. Mater. 133 (2006) 226–232.
[14] K.K. Ioannis, A.A. Triantafyllos, TiO_2-assisted photocatalytic degradation of azo dyes in aqueous solution: Kinetic and mechanistic investigations: A review, J. Appl. Catal. B: Environ. 49 (2004) 1–14.
[15] R. Saien, A.R. Soleymani, Constrain in solving Langmuir–Hinshelwood kinetic expression for the photocatalytic degradation of auramine O aqueous solutions by ZnO catalyst, J. Hazard. Mater. B 75 (2007) 245–247.
[16] B. Pare, P. Singh, S.B. Jonnalgada, Artificial light assisted photocatalytic degradation of lissamine fast yellow dye in ZnO suspension in a slurry batch reactor, Indian J. Chem. Technol. 232 (2010) 80–90.
[17] B. Pare, B. Sarwan, S.B. Jonnalagadda, The characteristics and photocatalytic activities of BiOCl as highly efficient photocatalyst, J. Mol. Struct. 2012 (1007) 196–202.
[18] W.F. Jardim, S.G. Moraes, M.M.K. Takiyama, Photocatalytic degradation of aromatic chlorinated compounds using TiO2: Toxicity of intermediates, Water Res. 31 (1997) 1728–1732.
[19] K. Vinodgopal, I. Bedja, S. Hotchandani, P.V. Kamat, A photocatalytic approach for the reductive decolorization of textile azo dyes in colloidal semiconductor suspensions, Langmuir 10 (1994) 1767–1771.
[20] M.A. Tariq, M. Faisal, M. Saquib, M. Muneer, Degradation of an anthraquinone and a triphenylmethane dye derivative in aqueous suspensions of semiconductor, Dyes Pigm. 76 (2008) 358–365.
[21] T. Jin, D. Sun, Y. Su, H. Zhang, H.J. Sue, Antimicrobial efficacy of zinc oxide quantum dots against *Listeria monocytogenes*, *Salmonella enteritidis* and *Escherichia coli*, J. Food Sci. 74 (2009) 46–52.
[22] B. Li, B.E. Logan, Bacterial adhesion to glass and metal oxide surfaces, Colloids. Surf. B 36 (2004) 81–90.